

Multimodal Optimal Score Level Fusion Method In Multimodal Biometric System

T. Srinivasa Rao^{1*}, Dr. E. Srinivasa Reddy ²

^{1*}Research Scholar, Acharya Nagarjuna University, Guntur, A.P., India & Professor, CSE, ACE
Engineering College, Hyd., India

²Professor & Principal, Acharya Nagarjuna University College of Engineering, ANU, Guntur,
A.P., India

¹<https://orcid.org/0000-0002-3766-7891>

ABSTRACT

An invariable mix of Biometric recognition as well as authentication process is used in almost every application for prevention of unauthorized access to computing resources. Though several research initiatives have been undertaken in recent years for making biometric algorithms more accurate for various kinds of features, they have largely ignored the critical aspects like reliability and robustness. Typically, information from multiple modalities is fused in a Multimodal biometric system to counter the shortcomings an individual classifier. This work primarily seeks to make optimum integration of biometric traits viz., iris, fingerprint and finger vein that have great complementary relation among them. It is basically done through optimization of performance in every single classifier through a novel Search Optimization Algorithm with backtracking function. Moreover, it tries to resolve conflicting beliefs affecting individual classifiers through use of proportional conflict redistribution rules, before obtaining a concurrent solution. Optimal behavior under a dynamic environment is shown in this system, either by boosting or, even by suppressing concurrent classifiers, thereby ensuring that classifiers do not have any more issues between them. The suggested multimodal system is developed by applying multimodal datasets generated using benchmarked digital imagery. Our system performs better averaging precision at 98.43% having 1.57% EER, thereby outperforming the existing techniques and promising to develop an advanced multimodal biometric system in subsequent efforts.

1. Introduction

Biometric systems cater to the dynamic security needs of the digital world. With usage in user recognition, they are also applied in critical authentication issues [1]. They have specific usage in

personal identification, banking, forensic, defense, and supervision. Suitable applications are created from human traits for biometric systems. In general, physiological, and behavioral traits are two facets of human traits [2]. Biometric recognition systems like Unimodal systems use just one modality to authenticate, besides uniquely identifying a person but have limited ability to address security challenges, thereby failing to protect from spoofing. Additionally, physical, and environment issues like noise-filled sensor information as well as tinier sample sizes reduce their ability to recognize accurately and perform, thereby possibly rendering them unreliable [3]. The dependence on a particular trait for a functionality makes a unimodal system ineffective while identifying some users with physical challenges. In such a scenario, by fusing different traits, it has emerged as a viable approach. Traits like fingerprint, face, vein, ear and iris fall in the realm of physiological wherein a fine-grain pattern is extracted. On the contrary, some traits in the behavior realm include walking, posture, voice, signature, and handwriting etc.

Complementary features, which are frequently collected from several modalities, are used in Multimodal biometric systems. Unlike unimodal systems, a multimodal biometric system provides high system dependability and durability in dynamic contexts, but also provide security against spoofing attacks. For instance, fingerprints are a common feature for identification and verification. However, when dealing with distorted photographs, scars, dead cells or wounds, unclean or greasy image sensor surfaces, and so on, identification systems relying exclusively on fingerprints might suffer. Furthermore, spoofing techniques, such as the use of counterfeit gummy fingers, may cause fingerprint-based devices to work poorly or fail. The finger vein feature, unlike a fingerprint, is derived from intra-derma patterns. The unimodal biometric systems using finger veins resist template forgery, though fail to solve biometric problems, including universality and temporal invariance [4]. Similarly, some discussion is mentioned on unimodal biometric system having iris characteristics [5]. Iris-based biometric devices identify the iris' distinct texture, which includes crypts, freckles, furrows, and corona. Furthermore, it is exceedingly uncommon that two people's iris patterns are similar [6]. Unimodal biometric systems that rely solely on facial traits gain attributes that humans use to identify other people [7]. The fundamental benefit of employing face characteristics is that it enables for contactless data collection, albeit this data can alter over time owing to ageing, position variations, and lighting changes. In multimodal biometric systems, we effectively address issues like non-universality, allowing co-opting bigger samples. They can also limit imposters' ability in spoofing genuine biometric traits while sorting big biometric database. Low mistake rates and improved recognition accuracies are achieved by such systems and gain low susceptibility in varied environments and circumstances because of the usage of several modalities, resulting in greater system robustness and dependability. Furthermore, because to the difficulties of forging numerous features, overcoming the authentication process in a multimodal biometric system necessitates greater work. When such systems are tuned to dynamic situations, their overall performance improves, leading to lesser False Acceptance Rates as well as False Rejection Rates. As a result, most multimodal biometric systems outperform unimodal systems, making them essential for real-world biometric applications.

Furthermore, a multimodal system's performance and usability may differ depending on the type of operation done, such as acquiring various modalities or fusing multiple modalities [8]. Multimodal biometric systems are of two types based on processes used to obtain various qualities: a) multi-sensor with multiple traits and b) single sensor with multiple traits [9]. Despite multimodal biometric systems solve the limitations of unimodal systems, they nonetheless provide annoyance to the user during registration and modality acquisition. Furthermore, multimodal biometric systems are created by fusing different modalities/levels i.e. properties, decision and score.

The suggested study introduces a multimodal biometric system to initiate effective decisions in separating a genuine subject from the impostor subjects, while the basic fusion approach acts as an automated tool for accurately identifying the real from imposter users.

The suggested score-based fusion approach is designed to get the best possible solution combining data with complementing traits like fingerprint, iris, and finger veins. Furthermore, the suggested approach considers the compatibility of the improved source classifier before finalizing authentication, which is highlighted below:

- Multimodal biometric system proposed with, finger veins, fingerprints and iris;
- Optimized function through Backtracking Search Optimization Algorithm (BSA).
- Conflicts among classifier scores resolved by applying Optimal score level fusion method; and
- Performs accurately with minimum faults as exhibited in results.

The relevant background study in multimodal biometric systems is presented in section 2, besides work motivation. Section 3 discusses multimodal system methodology. Also, this section shows estimating individual classifier scores and optimizing performance, besides showing core fusion method design. Section 4 shows its implementation on databases. In section 5, proposed system is compared with others. The summary and future projections in multimodal biometric system are presented in section 6.

2. Previous Work and Motivation

A number of researchers have studied unimodal biometric systems to overcome their shortcomings, through multimodal biometric systems by combining modalities such as features, scores, and decision. Strategy using score is dependent on triangular norm having four finger biometric features as multimodal biometrics, as compared to a combination of two or three traits in prior approaches [10]. The scores generated out of fingerprints, finger vein, knuckle print, and palm print features were combined using binary operations in this study. A multi-instance fusion approach for Finger-Knuckle-Print (FKP) identification [11] was presented on an equal level by integrating an individual's left index/middle fingers and right index/middle fingers at the matching score level. As a result, an odd face and iris picture was applied to a score level fusion approach [12] to solve the universality feature of a biometric system. This approach combines similar scores sourcing facial and iris classifier using weights. Another discussion was on multimodal biometric system dependent on facial and iris feature [13]. A combined sparse model powered multimodal biometric system[14] showed how to utilize the quality of obtained data to weigh modalities, while handling non-linearity through kernels. It directly evaluated translation of singular classifier

scores as belief masses [15], without the phase of merging classifier values. The rank level fusion utilizing the Markov chain also had a similar vein [16]. The biometric features of the face, iris, and ear were utilized to obtain the rankings of the individual classifiers. Multistage score level fusion integrated scores of various classifiers. By turning classifier scores into posterior probabilities at the normalization step, non-parametric score-based multistage was suggested to preserve orders in multimodal biometric systems [17], besides a user-specific and selective fusion mechanism in another [18]. A quality indicator bettered a multimodal fusion approach on scores[19]. In a similar vein, a fusion paradigm is shown to incorporate quality indicators in multimodal biometric fusion[20].

As opposed to biometric system functioning in fixed convolution points in some specified security scenarios, multimodal biometric system's adaptability has been found superior [21]. This approach, however, was unable to resolve contradiction in match score. Modalities have been fused at the deciding stage, in contrast to score level fusion, though it fails to have enough data to attain precision [22]. The suggested study aims to solve this challenge by developing an optimum fusion approach for high-security applications. We have evaluated three complementing modalities in the proposed work: iris, fingerprint, and finger vein that were picked up based on user preference as well as the availability of low-cost equipment. Because a biometric system can collect both a finger vein and a fingerprint simultaneously using a single image-capturing device [23], these characteristics together make biometric system less cost-effective and inflexible as well as exceedingly difficult to circumvent. Furthermore, fingerprints and finger veins have complementing features as shown in previous investigations [24]. The iris design was chosen as the third modality because of its resilience to ageing and toughness to forging. As a result, our multimodal biometric technology is extremely safe, reliable, and cost-effective. The optimum fusion of human senses in dynamic contexts, where separate senses come to make up others' inadequacies, was also explored [25].

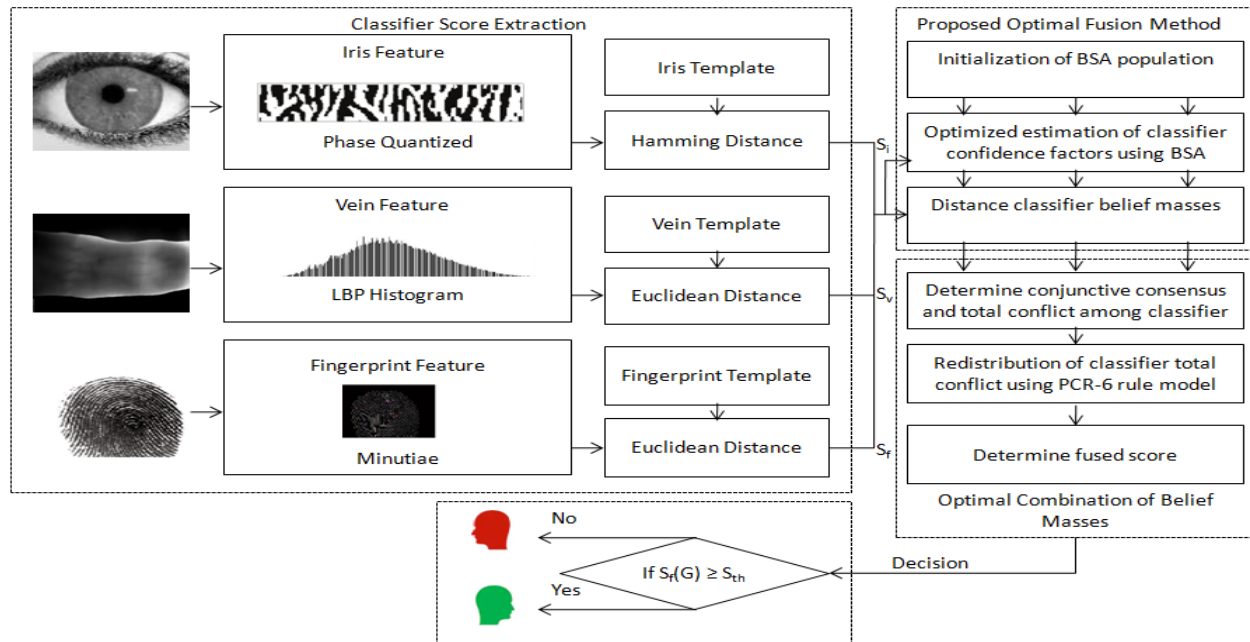


Fig.1 Proposed Multimodal Biometric Framework

3. Methodology for Proposed Multimodal Biometric System

Here, we present an ideal match comprising complementing biometric qualities viz., fingerprints, finger veins for multimodal biometric systems. Figure 1 exhibits comprehensive framework. The given data gets collected from such modalities to extract the associated features, as shown above. The rectangular iris sheet is extracted from the acquired eye picture using Daugman unwrapping that is then processed with 1-D log Gabor wavelets at multiple angles. For stages $[0-\pi/2)$, $[\pi/2-\pi)$, $[\pi-3\pi/2)$, $[3\pi/2-2\pi)$, the Gabor transform output is further transformed into phase sized portions. As a result, each Gabor transform pixel value gets two bits. These bits serve as the acquired iris trait's feature vector. On the acquired image, the Gabor transform is applied, and the result is separated as stand alone rectangular blocks. Each block's LBP histogram gets calculated, and the retrieved histograms are concatenated to generate ultimate features to be applied to finger veins. The fingerprint characteristic is drawn from collected image as minutiae. To get an accurate fingerprint feature vector, the collected incorrect minutiae points are filtered. Finally, match scores S_i , S_v and S_f are calculated by comparing the retrieved feature vectors to their respective templates. For optimal combination, the scores are also processed utilising suggested fusion approach. The optimal fusion approach uses a unique PCR-6 rule to merge the received scores after applying a discounting function to them. The Fusion approach is divided as classifier score optimization and optimum belief mass. Backtracking Search Optimization Algorithm obtains optimal weight for each classifier. The anticipated match scores are based on these weights, which operate as confidence factors. Using ideal confidence factors, the Denoeux approach is utilised to transform match scores into belief masses.

DSm T-based PCR-6 rule technique is applied to belief masses for solving problems in singular classifier beliefs.[26]. Each classifier's conflict and consensus is calculated in totality. The whole conflict, which is made up of six components branch off into three classifiers. Then, the final belief mass calculation is made for the system and comparison between final belief mass and threshold values is done in last belief masses. In a variety of cases, the suggested system behaves optimally. In the case of concurrent classifiers, for example, classifiers are either boosted or suppressed. Our fusion technique uses novel conflict resolution for discordant classifier sets. Latter subsections provide full design of the suggested fusion approach, as well as feature extraction methodologies.

3.1 Feature Extraction

Iris, fingerprint, and finger veins were selected for their compatibility and easy collection. We have used the method [16] for extracting iris features. Due to accurate localisation of the iris area, this approach provides great accuracy. First, the acquired ocular picture is localised for the desired location. On the region of interest, the Rubber sheet technique [27] is employed. Additionally, 1-D log Gabor wavelets are used to convolve the retrieved unwrapped iris picture. A circular ring is shown on the iris pattern in all rows, and 2-D iris picture is put through convolution row by row. Before being converted to phase-quantized bits, the convolved pattern is filtered for noise. The hamming length separating the acquired phase-quantized bits from the stored template estimates iris classifier potential. S_i Eq (1) is used to calculate the probability of an iris classifier (1).

$$S_i = \frac{|T_{ic} \odot T_{is} - HD_{s,c}|}{T_{ic} \odot T_{is}} \quad \dots (1)$$

Wherein $[HD]_{(s,c)}$ denotes the hamming distance, which is determined in Eq (2). The iris templates, both clicked and saved are represented by T_{ic} & T_{is} .

$$HD_{s,c} = T_{ic} \oplus T_{is} \quad \dots (2)$$

We used the method described in [10] to extract finger vein features. Due to its excellent vein filtering design, this approach achieves great accuracy. The Gabor Binary Pattern map is created by normalising and filtering the collected finger vein picture with Gabor Wavelet Kernels (GMP). Individual local binary pattern (LBP) histograms are calculated from the GMP map, which is partitioned into non-overlapping rectangular blocks. The final finger vein feature vectors concatenate LBP histograms. The probability of the finger vein classifier is calculated using the LBP histogram of the acquired vein picture and the LBP histogram of the saved templates stated here Eq (3).

$$S_v = \sum_r \frac{\sum_u \sum_v \min(h_{x,y,z}^s, h_{x,y,z}^c)}{\sum_u \sum_v h_{x,y,z}^s} \quad \dots (3)$$

Where, $h_{x,y,z}^s$ is the LBP histogram of stored template and $h_{x,y,z}^c$ is the LBP histogram of captured image for scale x and y directions and z. The minutiae extraction approach provided by authors [28] is used to extract features from fingerprints. Also, as proposed in [29], erroneous minutiae get refined through methods using fuzzy rules. By calculating threshold distance from one termination to another as well as angle variations in synchronised paths, erroneous minutiae are deleted. While efficiently leveraging ridge ends and bifurcations, the algorithm creates standard minutiae matches after acquiring the valid minutiae. The fingerprint minutiae pattern comes into consideration while

matching retrieved characteristics. Using Eq (4), fingerprint feature similarities are calculated like a match score[17].

$$S_f = \frac{N_{match}^2}{N_s N_c} \quad \dots (4)$$

N_{match} denotes the number of matched minutiae pairings, whereas N_s, N_c denote overlapping minutiae in the templates clicked and saved. To reach best choice, the predicted likelihood values for three classifiers S_i, S_v and S_f are submitted to the suggested adaptive score based fusion approach. The suggested fusion method's basic design is detailed in the next part.

3.2 Proposed Fusion Method

Multimodal fusion makes optimum decisions possible. We present two-layered optimum fusion approach to integrate scores out of three attributes in this paper. The data fusion approach enhances and inhibits concurrent classifiers, though conflicts are successfully resolved between discordant classifiers.

3.2.1 Stage I: Classifier Score Optimization

The suggested fusion technique begins with the optimization of individual classifiers. For this, we used Shafer's Method having frame of discernment, $\Theta = \{G, I\}$, specified over two exclusive focus elements to change the fusion issue. For corresponding classifiers, the focal element describes the genuine and impostor classes. Individual classifier scores S_i, S_v and S_f , Eq. (1, 3, 4), are transformed to belief masses utilizing Denoeux belief [30] through Eq (5, 6).

$$m_x(G) = k * \Psi(S_x) \quad \dots (5)$$

$$m_x(I) = 1 - k * \Psi(S_x) \quad \dots (6)$$

Wherein, $m_x(G)$ is the bonafide class belief mass, $m_x(I)$ is the imposter class belief mass, $x \in i, v, f$ and Ψ is a sigmoid function applied to map scores (0,1). In iris, finger vein, and fingerprint classifiers, the confidence factor k is calculated. The Confidence elements are best chosen based on their score value. Not only does choosing the right confidence factors help with score to mass conversion. It fires up classifier as well as containment. BSA [31] promises to solve the drawbacks of slow computing and premature convergence, is used to find the optimal values of confidence factors. In BSA, steps consist of initialization, selection-I, selection-II, mutation and crossover. A colony size $N=200$ is defined in initialization step through Eq. (7).

$$p_y \sim U(0,1) \quad \dots (7)$$

Wherein, U denotes equated distribution of population across the range (0, 1) and $y \in \alpha, \beta, \gamma$, which is done to generate initial populations p_α, p_β & p_γ for confidence factors α, β and γ . Later, generation of belief masses for each population elements of the classifiers is done by using Eq. (8).

$$mass_y = p_y * S_x \quad \dots (8)$$

Also, Eq. (9) is used to determine a fitness value F_y^p for each population element in the initialization step of BSA, which is dependent upon false acceptance and false rejection costs and the following rate values.

$$F_y^p = C_{fa} * FAR_y^p + C_{fr} * FRR_y^p \quad \dots (9)$$

Where, F_y^p represents fitness values of an element p of the population p_y for $y \in \alpha, \beta, \gamma$. While C_{fa} is cost of false acceptance, C_{fr} is the cost of false rejection. Also, FAR_y^p is the false acceptance rate and FRR_y^p is false rejection rate for an element p of the population p_y . In initial stages, the historical population p_y^{old} is defined for each classifier by using uniform distribution as presented in Eq. (7). The historical populations of each classifier are updated in the selection-I stage. It is attained by generating two random matrix r_1 & r_2 of size $N \times 1$ over the range (0, 1) using Eq. (10):

$$\text{If } r_1 < r_2, \text{ then, } p_y^{old} = p_y | r_1, r_2 \sim U(0,1) \quad \dots (10)$$

Offspring population O_y is created for p_y in mutation step by applying pre-outlined scaling factor S in Eq. (11).

$$O_y = p_y + (\text{map} * S) * (p_y^{old} - p_y) \quad \dots (11)$$

Wherein map denotes random matrix created across value range (0, 1). Offspring is optimised in the crossover operation by applying boundary control techniques to reduce offspring elements. The offspring populations are given the fitness value F_y^o . These fitness values are used to update the parent populations as a deciding factor. The offspring elements of low fitness values take the pace of matching parent population elements in the selection-II procedure, as shown in Eq (12).

$$\text{If } F_y^o < F_y^p \text{ then } p_y = O_y \quad \dots (12)$$

Each classifier's parent population element of lowest fitness values get calculated iteratively. In iris, finger vein, and fingerprint classifiers, global-fit components get determined as confidence factors with ideal values i.e. α, β and γ , respectively. Eq. 1 is utilised to transform classifier scores through optimal confidence factors as belief masses (5, 6). In addition, as explained in the following stage.

3.2.2 Stage II: Optimal Combination of Belief Mass

Shafer's Method is used to solve the multiple classifier fusion issue, using a frame of discernment of $\Theta = \{G, I\}$ specified across two focus elements. Independent features are considered while combining belief masses for a frame of discernment. PCR-6 principles based on Dezert-Schmarandche Theory (DSm T) [26] are used to integrate these masses. The PCR-6 approach is a series of guidelines for resolving disagreement between sources of information that are highly inconsistent. It entails calculating conjunctive consensus, partial conflict, and total conflict. The partly conflicting masses are transferred to the focal elements that correspond to them. The suggested fusion approach is based on a three-source system, $S = \{i, v, f\}$. Eq. (13) is applied to determine common agreement between all masses on choice of focal element G as $m_{cc}(G)$.

$$m_{cc}(G) = \prod_{K=1}^N m_{S(K)}(G) \quad \dots (13)$$

Where, $N = 3$ stand for sources, while total conflict among belief masses i.e. $m_{tc}(G \cap I)$ gets determined through Eq. (14), consisting of six partial conflicting masses.

$$m_{tc}(G \cap I) = \sum_{j=1}^2 m_{S(1)}(Y_j) \sum_{\substack{\cap_{n=2}^N Y_j \cap Y_{S(n)} = \emptyset \\ (Y_{(j)}, Y_{S(N)} \in \Theta)}} \prod_{K=2}^3 m_{S(K)}(Y_{S(K)}) \quad \dots (14)$$

Redistribution of such partial conflicting masses are done proportionate to mass of focal elements creating pool of total conflicts through Eq. (15).

$$m_{rd}(G) = \sum_{\substack{k=1 \\ G \in \Theta}}^3 m_{S(k)}(G)^2 \sum_{\substack{\cap_{n=1}^{N-1} Y_{Y_{\sigma_k(n)}} \cap G \equiv \emptyset \\ (Y_{\sigma_k(n)}, \dots, Y_{\sigma_k(n-1)}) \in \Theta}} \left[\frac{\prod_{j=1}^2 m_{S(\sigma_k(j))}(Y_{S(\sigma_k(j))})}{m_k(G) + \sum_{j=1}^2 m_{S(\sigma_k(j))}(Y_{S(\sigma_k(j))})} \right] \dots (15)$$

Where, $m_k(G) + \sum_{j=1}^2 m_{S(\sigma_k(j))}(Y_{S(\sigma_k(j))}) \neq 0$ and value of $\sigma_k(j)$ is calculated through Eq.(16)

$$\sigma_k(j) = \begin{cases} j, & \text{if } j < k \\ j + 1, & \text{if } j \geq k \end{cases} \dots (16)$$

Lastly, final belief mass is determined by adding redistributed masses conjunctive consensus and create genuine class i.e. $S_f(G)$ through Eq. (17).

$$S_f(G) = m_{rd}(G) + m_{cc}(G) \dots (17)$$

The belief mass $S_f(G)$ is contrasted to the ideal threshold value S_{th} in the decision technique to arrive at a final choice. For a biometric system to achieve high accuracy, the ideal value of S_{th} must be estimated. Any departure from the ideal value may cause the biometric system's accuracy and reliability to suffer. A lower threshold value than its optimal value leads to a larger number of false acceptances, resulting in a high FAR. On the other hand, choosing a higher threshold value than the optimum value results in many erroneous rejections, resulting in a high FRR. To minimise excess error of any such sort, the ideal threshold value S_{th} is chosen as the value at which the system attains equated erroneous acceptance and false rejection (Equal Error Rate). The optimum threshold value S_{th} found for experimental validation in the proposed study is 0.53.

Algorithm 1 Proposed Multimodal Biometric System

[Genuine, Imposter] = Multi modal_System [Image_i, Image_v, Image_f]

1. Identify feature vectors viz. $T_{ie}, h_{x,y,z}^c, N_c$.
 2. Attain similarity scores viz. S_i, S_v, S_f using Eq.(1), (3), & (3).
 3. **Stage I:** Classifier Score Optimization
 - i. Identify belief masses $[m_i(G), m_v(G), m_f(G)]$ using Eq.(5)
 - ii. Initialization: Decide parent populations $[p_\alpha, p_\beta, p_\gamma]$ using Eq.(7)
 - iii. Identify mass values $[mass_\alpha, mass_\beta, mass_\gamma]$ using Eq.(8)
 - iv. Allocate fitness values $[F_\alpha^p, F_\beta^p, F_\gamma^p]$ using Eq.(9)
 - v. For $z=1 : 1000$
 - a. Choice I: Randomly update historic populations $[p_\alpha^{old}, p_\beta^{old}, p_\gamma^{old}]$ using Eq. (10).
 - b. Mutation + Crossover: Determine offspring populations $[O_\alpha, O_\beta, O_\gamma]$ using Eq. (11).
 - c. Choice II: Update p_α, p_β & p_γ using Eq. (12).
 - d. Identify element of p_α, p_β & p_γ with minimum fitness.
 - End
 - vi. Calculate global fit elements $[\alpha, \beta, \gamma]$ from $[p_\alpha, p_\beta, p_\gamma]$
-









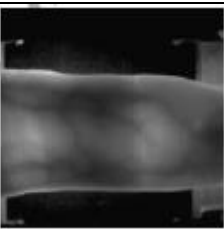
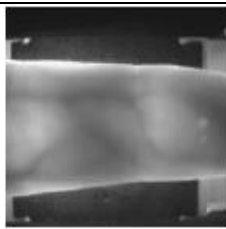
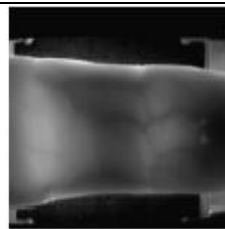

-
4. **Stage II:** Optimal combination of belief masses
 - a. Create Conjunctive Consensus and Total Conflict by using Eq. (13) &(14).
 - b. Redistribute partial conflict by using Eq. (15).
 - c. Identify total belief of genuine focal element $S_f(G)$ by using Eq. (17).
 5. **Decision Method:**
 If $S_f(G) \geq S_{th} \text{Genuine}$
 Else Imposter
-

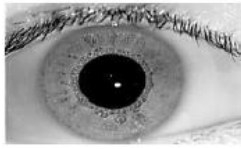
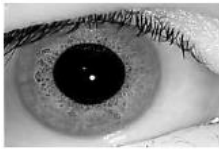


Algorithm 1 is the pseudo code applied in this biometric recognition system. Experiments using benchmark datasets were done to validate the suggested technique. The next part goes through the datasets in depth as well as the implementation of the suggested approach.

4. Databases and Experimental Design

The proposed approach is validated using multimodal datasets collected from several standard datasets created by combining datasets viz., IITD Poly U Iris database [32], VERA finger vein database [33], FVC 2006 fingerprint database [34] & CASIA fingerprint database (CASIA-FingerprintV5, <http://biometrics.idealtest.org/>). Many biometric systems are extensively tested using them [4,14, 21]. Table 2 shows examples of photos from various datasets.

Table 2 Sample images for Experimental Dataset extraction

Database	Sample Image			
Fingerprint				
	CASIA Fingerprint Database (CASIA-FingerprintV5)			
				
Finger Vein	FVC 2006 Fingerprint Dataset			
				

	VERA Finger vein Database			
Iris				
	IITD Poly UIris database			

The IITD Poly U iris database is made up of photos taken with a digital CMOS camera inside. Each patient has 5 photos of their left and right eyes in the collection. Each picture is 320x240 pixels in size. The CASIA fingerprint database contains many photos of each subject's finger taken at various angles. Each picture is 328x356 pixels in size. The FVC2006 fingerprint database comprises the fingerprints of 140 people. For each subject, it comprises of 12 photos obtained at various angles. Each picture is 96x96 pixels in size. The VERA finger vein database has 6 photos of the index, middle, and ring fingers for both the left and right index fingers, with a total of 110 users. The images in this gallery are a mix of interior and outdoor shots. Each picture is 665 x 250 pixels in size.

In the experimental validation section, this multimodal biometric system is verified using datasets- Datasets 1 & 2. Dataset 1 brings together 50 samples from the IITD PolyU Iris dataset, the VERA finger vein dataset, and the CASIA fingerprint dataset. Initially, 50 separate iris dataset subjects are allocated to 50 distinct finger vein dataset subjects. Furthermore, the subjects of the previously combined dataset are assigned to 50 different fingerprint dataset subjects. As a result, a virtual multimodal dataset with 50 unique subjects is created. Dataset 2 is created in the same way, using 50 unique participants from the IITD Poly U Iris dataset. The subjects selected for Dataset 1 are mutually exclusive with those selected for Dataset 2. To obtain fivefold cross validation of results, we randomly selected five picture samples from the above mentioned benchmark datasets for each subject of Dataset 1 and Dataset 2. In addition, we created a 100-subject consolidated dataset by combining subjects from Datasets 1 and 2.

On the MATLAB 13.1 platform, the suggested biometric system is built. The Intel i5 CPU and 8 GB RAM are installed on the hardware platform. The computing time for 50 images during 35 iterations remains 53 seconds, implying that each identity authentication takes 30 milliseconds on average. We ran 35 iterations of the suggested technique for experimental simulation to address the stochastic character. The BSA method optimises classifier scores, which results in a low computing need. This shows how the planned biometric system works in real time. Furthermore, the suggested biometric system's experimental findings are acquired using 5-foldcross validation. For this, each subject's sample is separated into four enrolment samples and one test sample. This technique is performed five times to ensure that each sample is utilised just once as the test sample. Average values across 5 rounds are reported in the next section as experimental findings. The reproducibility of experimental results produced across a restricted dataset is assessed using 5-fold cross validation. Next, the details of the suggested method's validation are discussed.

5. Experimental Validation

On chimeric multimodal datasets, the suggested multimodal biometric system is tested qualitatively and quantitatively. In qualitative analysis, the suggested multimodal fusion method's performance is shown by generating optimal confidence factors and integrating modalities to generate the final score. Individual classifiers are compared to the proposed technique using distributions of genuine class scores and impostor class scores. Furthermore, performance measurements i.e. Receiver Operating Curves (ROC), Equal Error Rate (EER), Decidability Index, and Standard Deviation are used to analyse the system objectively. The suggested method's performance is also compared to those of state-of-the-art fusion approaches.

5.1 Qualitative Analysis

Using chimaera datasets, this multimodal system is tested in terms of quality paradigm by exhibiting the suggested biometric system's score level fusion as well as the distribution of scores for authentic as well as impostor classes.

5.1.1 Demonstration of Proposed Optimal Fusion Method

For an ideal combination of three classifiers, the suggested fusion approach has two steps. Figure 2 depicts the optimal creation of confidence factors as well as the fusion of belief masses. The change in confidence factor regarding matching score values is displayed in Fig. 2a and Fig. 2b for finger vein and fingerprint classifiers. High score values (greater than 0.5) result in high confidence factors, as seen in Fig. 2a. As a result, greater believing masses emerge. Low confidence factors are found for low match score (0.4) values, as shown in Figure 2b. A score of 0.65 (>0.5), for example, indicates a higher confidence factor. As a result, a big belief mass is produced by a high confidence factor resulting in higher score values. Low score values, on the other hand, result in a low confidence factor, which leads to a tiny belief mass. The score dependent fitness function is primarily responsible for the adaptive character of the confidence factor with different score values.

Furthermore, the suggested fusion method's Stage II is applied to belief masses to better the current classifiers, as well as resolve conflicts in discordant classifier, Figures 2c and 2d demonstrate conflict resolution among belief masses for discordant classifiers. The higher belief masses from contemporaneous classifiers likely to generate huge, fused masses in real people. big belief masses come from single classifiers bolster ultimate belief mass by confirming a subject's genuineness. For instance, due to classifier concurrence, the final fused mass of subject 14 (shown in Fig. 2c) is higher than the equivalent classifier belief masses. This is an example of people's beliefs being boosted. Similarly, when all the classifiers agree that the topic is not legitimate, the final fused mass is suppressed. Last fused mass becomes substantially smaller than separate classifier belief masses, as seen in Fig. 2d. Conflicting classifier masses are calculated in Eq. (14), before shared to single components as per their share in conflicts in the event of discordant classifiers.

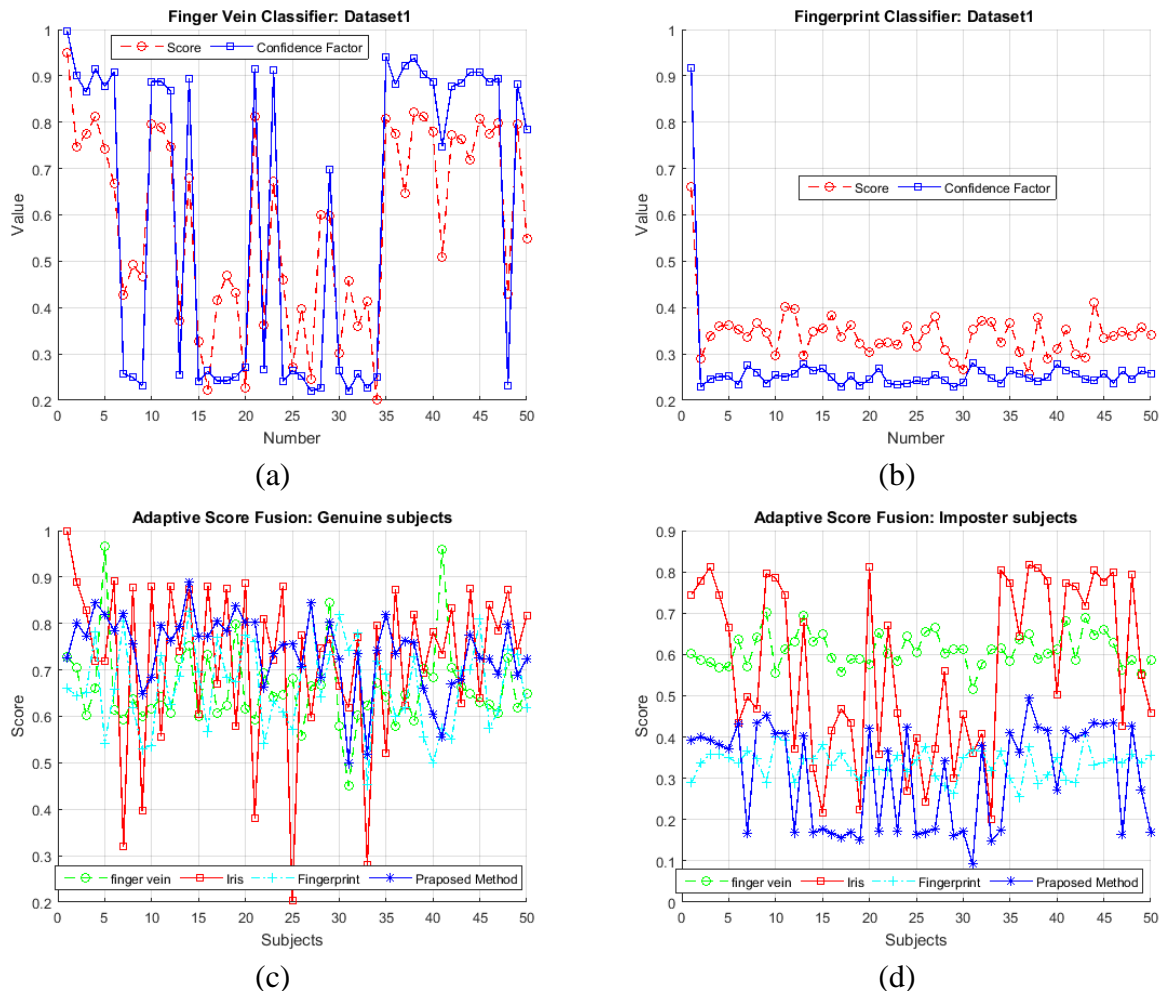
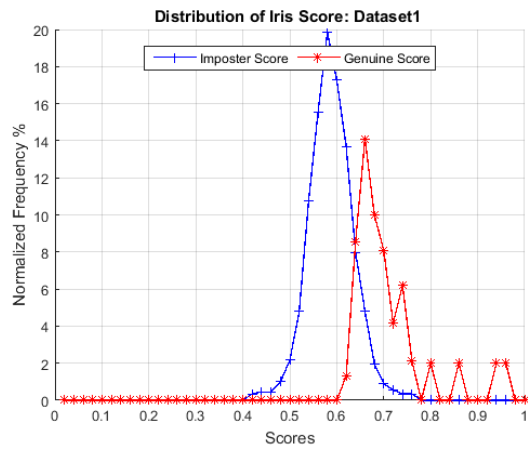


Fig. 2 Multimodal Fusion Method for Dataset1: a) Vein classifier confidence factor variation b) Fingerprint classifier confidence factor variation c) Genuine score fusion d) Imposter score fusion.

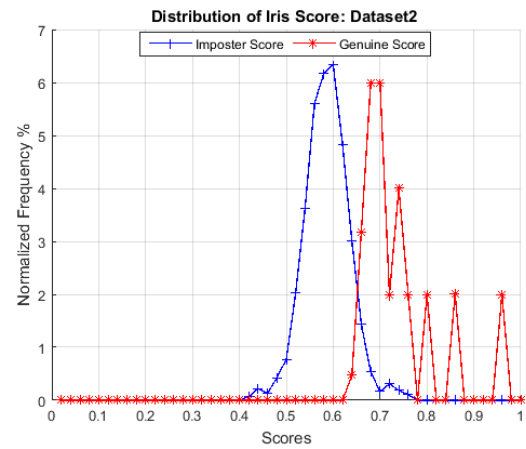
5.1.2 Demonstration of Classifier Performance Optimization

A two-stage integrated classifier improves singular classifier showing while combining belief masses appropriately. As a result, the ingenuine and impostor score distributions are more separated. For two datasets, we presented the score distributions of classifiers as well as the best fused score distribution in Fig. 3.

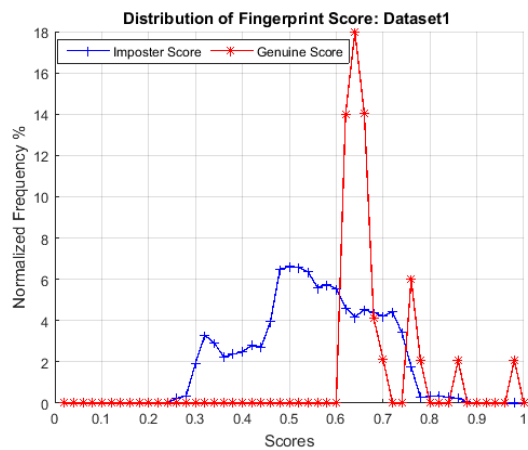
For the iris classifier, the score distributions into genuine and impostor classes overlap, illustrated as Figs. 3a and 3b. This merging of real and impostor score distributions is mostly due to iris shape anomalies, off-angle pictures, and blur. A little difference in class score distributions between real and impostor results in a higher false acceptance rate, reducing iris-based biometric system precision. The genuine and impostor score distributions for Dataset1 and Dataset2 are given in Fig.3c and Fig. 3d, accordingly, for the fingerprint classifier.



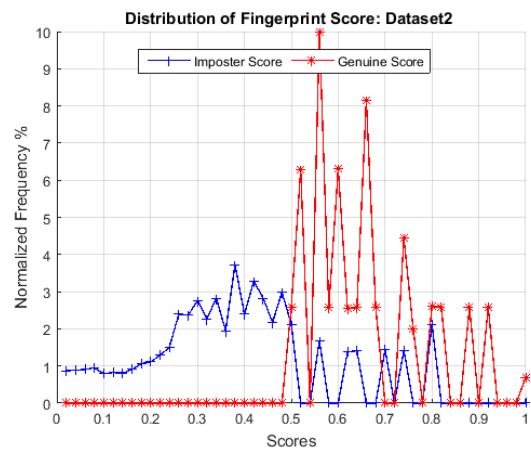
(a)



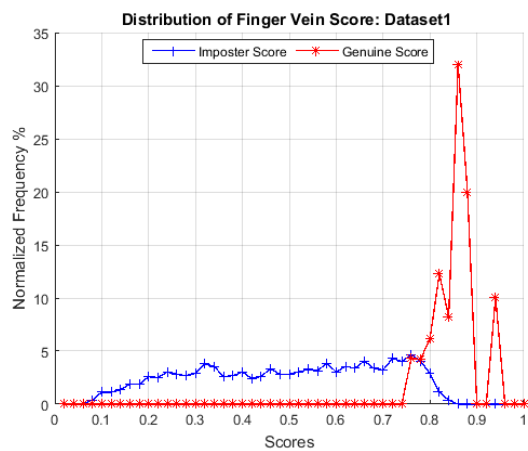
(b)



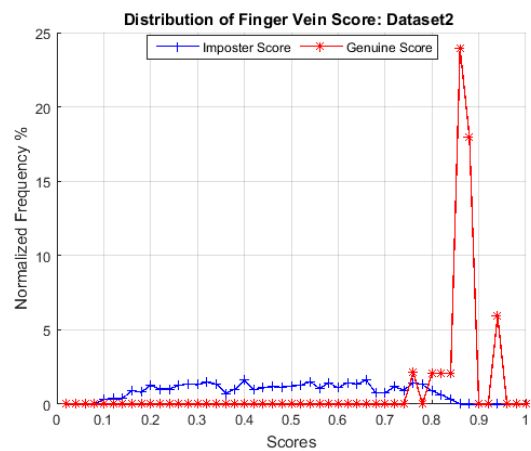
(c)



(d)



(e)



(f)

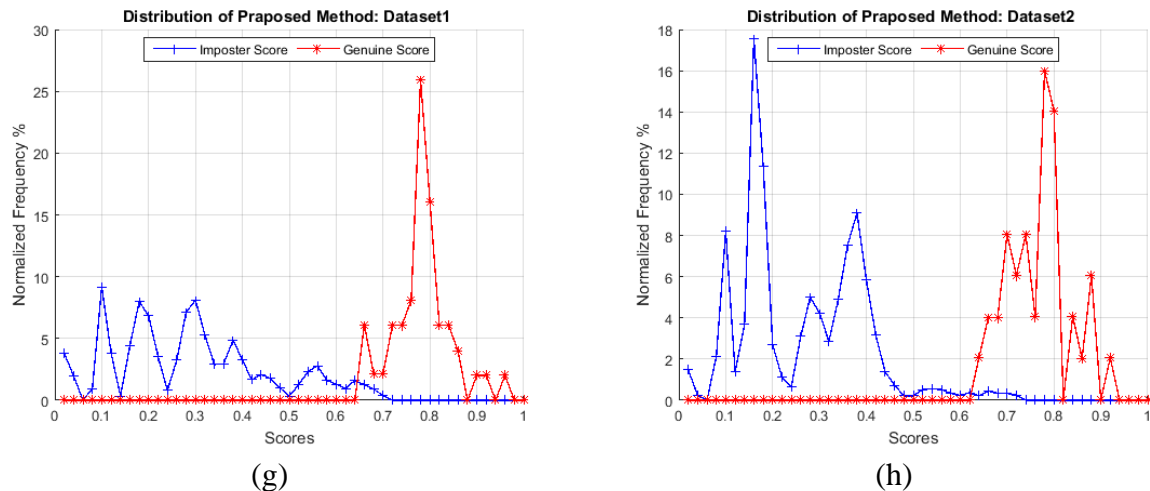


Fig. 3 Sample Score Distributions for Genuine and Imposter Class: a) Iris classifier for Dataset1 b) Iris classifier for Dataset2 c) Fingerprint classifier for Dataset1 d) Fingerprint classifier for Dataset2 e) Finger vein classifier for Dataset1 f) Finger vein classifier for Dataset2 g) New method for Dataset1 h) New method for Dataset2

The collected fingerprint pictures in Dataset 1 are not only without boundary information but affected by environment factors as well. As a result of these difficulties, the score distributions for the real and impostor classes tend to overlap. In Dataset 2, the modest mix between genuine and impostor score distributions for the fingerprint characteristic due to better fingerprints having unambiguous border information. Score distributions for genuine and impostor classes are displayed in Fig. 3e and Fig. 3f, respectively, for the finger vein classifier. Even though vein patterns beneath the skin are less impacted by external factors, the uniform distribution of impostor score is mostly due to mechanism for score calculation used by the finger vein classifier. As a result, the false acceptance rate and overall accuracy of the biometric system based only on finger veins suffers. Such genuine and impostor class score matrix for the suggested technique, on the other hand, are suitably separated, resulting in the best decision boundary for two classes. For Dataset1 and Dataset2, the score distribution separation for the suggested biometric system is displayed in Fig 3(g) and 3(h), accordingly. Quantitative examination of the decidability index will further enhance the vast separation of real and impostor class score distributions.

5.2 Quantitative Analysis

Here, the performance is additionally quantified using the decidability index and the Equal Error Rate (EER) to create quantitative score in comparison to state-of-the-art fusion approaches, such as: i) PSO-based weighted sum fusion (PSO-WS) [35]. ii) LFI (Local Feature Integration) (iii) The rule of Max [37] iv) Minrule [37] iv) Minrule [37] iv) Minrule (v) The Sum Rule (Rule 38) [39] (vi) Hamacher t-norm (Hm). We applied feature extraction and score estimation methods as stated in Section 3.2 to compare different fusion approaches as well as to evaluate unimodal methods.

Decidability Index: We employed the decidability index as a performance indicator to assess the difference in score distribution between the genuine and impostor classes. The Decidability Index is calculated in Eq. (24).

$$d = \frac{|\mu_g - \mu_i|}{\sqrt{\frac{(\sigma_g^2 - \sigma_i^2)}{2}}} \quad \text{--- (24)}$$

While μ_g and μ_i are the mean values of genuine and impostor scores, accordingly, σ_g and σ_i are the standard deviations of genuine and impostor scores. A classifier with a high decidability index can tell the difference between impostor and real subjects quickly. Table 3 lists the decidability values of individual classifiers. As previously stated, the low decidability index $d=4.804$ for the fingerprint characteristic corresponding to Dataset1 is mostly due to the lack of topic boundary information. High-quality fingerprint photos conversely, accounts for Dataset2's high decidability index of $d=10.047$.

Table 3 Decidability index of individual classifier

Classifier	Decidability Index	
	Dataset1	Dataset2
Fingerprint	4.804	10.047
Finger Vein	5.823	5.284
Iris	4.591	5.178

Because of the uniform score distribution in the case of impostor score, the decidability index for finger vein is low, at 5.823 for Dataset 1 and 5.284 for Dataset 2. In general, biometric systems that rely solely on finger veins struggle to discriminate between real and counterfeit participants. Likewise, the iris classifier's poor decidability index of 4.591 for Dataset 1 and 5.178 for Dataset 2 is mostly owing to inconsistencies in iris form, off-angle pictures, and blur.

Table 4 Decidability Index of Fusion Methods

Fusion Method	Decidability Index	
	Dataset1	Dataset2
PSO weighted fusion	9.562	14.351
LFI	7.646	10.082
Max	3.896	3.957
Min	3.332	3.815
Sum	4.121	4.134
Hamacher t-norm	1.095	1.130
Proposed Method	14.864	18.868

We evaluated the decidability index for the proposed method with alternative fusion strategies, in addition to comparing the decidability index for biometric features. Table 4 shows that the suggested fusion technique achieves a high decidability index of 14.864 for Dataset1 and 18.868 for Dataset2 by boosting or suppressing concurrent classifiers and resolving conflict among discordant classifiers. The enhanced performance of the fingerprint classifier, which is further augmented by additional modalities in a demanding setting, is ascribed to a comparably larger value for Dataset2. Other fusion approaches, such as LFI and PSO-WS, have a marginally higher decidability index than individual modality. PSO-WS calculates a final score via evolutionary PSO, which leads to optimal allocation. Similarly, for adaptive fusion of classifier scores, the LFI technique addresses classifier error. For the fusion methods Max, Min, Sum, and Hm, a low decidability index results in a high mistake rate and, as a result, low accuracy. In conclusion, the findings in Tables 3 and 4 show that our technique has the maximum decidability index, which leads to an effective categorization of real from impostor individuals. The suggested fusion method's optimal results are mostly due to the two-stage integration, in which classifier performance is improved in the first stage utilising BSA. The improved classifiers are merged in the second stage utilising PCR-6 rules based on DS_mT. Using the performance metric EER, the relevance of a high decidability index value for the suggested multimodal biometric system is also assessed.

Equal Error Rate: To assess the equal error rate of each fusion procedure, ROC curves are shown (EER). The Genuine Acceptance Rate (GAR) is displayed versus the False Acceptance Rate (FAR) for each fusion process in ROC curves, as illustrated in Fig. 4. The ROC curve for fusion techniques for Dataset1 shows that the suggested approach demands a high GAR value for a given amount of FAR, resulting in high accuracy, as illustrated in Fig.4a. Similarly, the ROC curve for Dataset2 in Fig. 4b shows that for a given FAR value, the suggested technique requires a high GAR value.

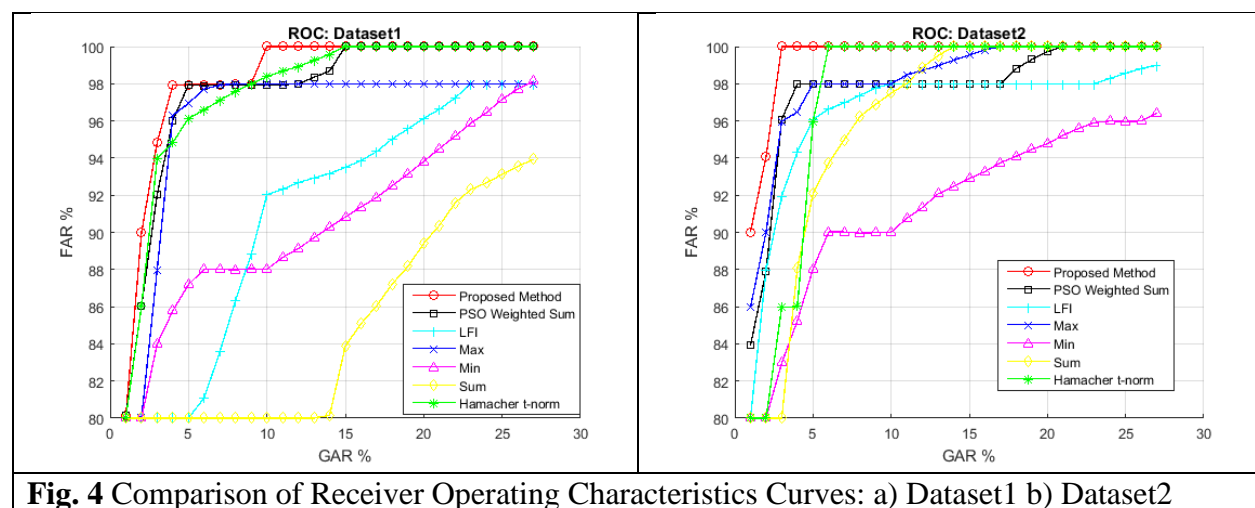


Table 5 shows the EER values for each examined fusion method. The EER values presented for the proposed fusion approach are average values acquired across 35 runs of the procedure to account for the stochastic nature of BSA. EER values for PSO-based weighted sum fusion (PSO-WS) are calculated as the average of 35 fusion technique runs. The deterministic nature of fusion techniques LFI, Max, Min, Sum, and Hm, on the other hand, makes it easy to receive results for even a single run of the algorithm. In addition, the EER values for a consolidated multimodal dataset have been established. The 50 separate individuals from Dataset 1 and 50 distinct people from Dataset 2 were combined to create this consolidated dataset.

Table 5 Comparison of EER values for Fusion Methods

Dataset	Proposed Method	PSO Weighted Sum	LFI	Max	Min	Sum	Hamacher t-norm (Hm)	Finger Vein	Iris	Fingerprint
Dataset1	2.28	2.53	7.78	3.01	9.80	13.01	3.81	14.46	18.23	15.91
Dataset2	1.00	1.99	3.60	2.79	8.52	4.75	3.41	14.01	17.48	10.33
Consolidated Dataset	1.57	2.02	5.44	2.92	9.16	8.94	3.65	13.22	17.82	12.64

The suggested strategy, as shown in Table 5, obtains the lowest EER value not only for Dataset 1, Dataset 2, but also for the consolidated dataset. This is in line with the suggested method's high decidability index. Fusion methods such as Max, Min, Sum, and Hm, on the other hand, have high EER values, owing to their deterministic fusion process and lack of classifier optimization. Although PSO-Weighted-Sum achieves classifier score optimization, it fails to resolve conflicts across classifiers, resulting in a high EER value. Furthermore, on a consolidated dataset, the suggested strategy outperforms conventional fusion methods. We calculated standard deviation in EER values acquired over 35 runs to address the stochastic aspect of the proposed fusion approach and PSO based weighted sum fusion (PSO-WS). Table 6 tabulates the standard deviation data. The suggested method's low standard deviation suggests EER, despite the proposed fusion method's stochastic character.

Table 6 Standard deviation of EER values

Dataset	Proposed Method	PSO weighted Sum
Dataset1	0.0601	0.0706
Dataset2	0.0321	0.0465

Consolidated Dataset	0.0537	0.0565
----------------------	--------	--------

To summarise, the complementing features are fused optimally utilising the suggested fusion approach, making the system flexible to dynamic settings. Individual classifiers are unable to efficiently discriminate between real and impostor classes, according to quantitative study. This is mostly owing to iris attributes' uneven shape and off-angle blur, as well as fingerprint and finger vein traits' lack of boundary information. The suggested fusion approach, on the other hand, mixes up single classifiers for negating their constraints. Inversely, it is reflected in the suggested method's high decidability index. Furthermore, new method's adaptive fusion is performed by optimising classifier confidence factors and resolving disputes among classifier scores. Competitive approaches, on the other hand, are unable to handle the issue of conflicting classifier results and are unable to adapt to changes in individual characteristic ratings. When compared to other competing approaches, this optimal behaviour is supported by a high decidability index of low EER. Furthermore, the suggested approach may be used in real-time for a variety of industrial and security applications due to its short calculation time. As a result, the proposed multimodal biometric system performs better thanks to individual classifier performance optimization, which is accomplished by either bettering or suppressing concurrent classifiers as well as resolving discordant classifier scores.

6. Conclusion and Future Direction

This paper offers a multimodal biometric system based on three complementing traits viz., iris, finger vein, and fingerprint, with finger vein and fingerprint collected concurrently using a single device. Boosting and suppression of concurrent classifiers, as well as resolution of conflict among discordant classifiers, are used to achieve optimal score level fusion. Shafer's approach with a frame of discernment, $\Theta = \{G, I\}$, defined over two exclusive focused elements is used to solve the score level fusion problem. The evolutionary Backtracking Search Optimization Algorithm is used to optimise the individual classifiers (BSA). Proportional Conflict Redistribution (PCR-6) rules are used to incorporate the classifiers' optimal belief masses. Other than its computational efficiency for integrating multiple scores, the suggested optimal score level fusion method never involves any classifier training. The large disparity in score distribution between the impostor and real classes contributes to the suggested biometric system's excellent accuracy and dependability. The suggested method is tested using chimaera datasets made up of benchmarked iris, finger vein, and fingerprint pictures. The suggested multimodal fusion approach performs better than fusion techniques in diverse challenging scenarios, in terms of comparative scores, both qualitatively and quantitatively.

While adaptive nature of multimodal biometric systems is dependent feature level fusion has been examined, it is difficult to accomplish adaptive nature of score-based fusion. We will examine include user-specific features and biometric quality as reliability variables in the suggested fusion approach in the future. Incorporating such skills into biometric fusion might potentially improve the system's adaptive nature, allowing it to deal with a wider range of difficulties, such as image

quality variance. User-specific features might be added for the convenience of the user or depending on the system's performance for a certain usage. The biometric quality of the collected traits can be used to estimate the trait's dependability. Importance and reliability can be used as weights for certain users and can be learnt over time to improve the system's dependability and robustness. The suggested biometric system may be expanded to incorporate security level adaptation.

References:

- [1] Ortiz, Nicolas, Ruben Dario Hernández, Robinson Jimenez, Mauricio Mauledeoux, and Oscar Avilés. "Survey of Biometric Pattern Recognition via Machine Learning Techniques." (2018).
- [2] Mordini, Emilio, and Dimitros Tzovaras, editors. Second generation biometrics: The ethical, legal and social context. Vol. 11. Springer Science & Business Media, 2012, 11, 49–79.
- [3] Cappelli, R., Ferrara, M. and Maio, D., 2012. A fast and accurate palmprint recognition system based on minutiae. *IEEE Transactions on Systems, Man, and Cybernetics, Part B (Cybernetics)*, 42(3), pp.956-962
- [4] Tao, Q., 2009. Face verification for mobile personal devices. University of Twente [Host].
- [5] Jain, A.K. and Kumar, A., 2012. Biometrics of Next Generation: An Overview, w: The Second Generation Biometrics: The Ethical, Legal and Social Context, E. Mordini, D. Tzovaras (red.).
- [6] Dainty, C., GONCHAROV, A., Corcoran, P. and Andorko, I., Fotonation Ltd, 2018. Optical system for acquisition of images with either or both visible or near-infrared spectra. U.S. Patent Application 10/051,208.
- [7] Walia, G.S., Raza, S., Gupta, A., Asthana, R. and Singh, K., 2017. A novel approach of multi-stage tracking for precise localization of target in video sequences. *Expert Systems with Applications*, 78, pp.208-224
- [9] Lumini, A. and Nanni, L., 2017. Overview of the combination of biometric matchers. *Information Fusion*, 33, pp.71-85
- [10] Peng, J., El-Latif, A.A.A., Li, Q. and Niu, X., 2014. Multimodal biometric authentication based on score level fusion of finger biometrics. *Optik-International Journal for Light and Electron Optics*, 125(23), pp.6891-6897.
- [11] Shariatmadar, Z.S. and Faez, K., 2014. Finger-Knuckle-Print recognition performance improvement via multi-instance fusion at the score level. *Optik-International Journal for Light and Electron Optics*, 125(3), pp.908-910.
- [12] Sim, H.M., Asmuni, H., Hassan, R. and Othman, R.M., 2014. Multimodal biometrics: Weighted score level fusion based on non-ideal iris and face images. *Expert Systems with Applications*, 41(11), pp.5390-5404.
- [13] Liao, H.F. and Isa, D., 2011. Feature selection for support vector machine-based face-iris multimodal biometric system. *Expert Systems with Applications*, 38(9), pp.11105-11111.

- [14] Shekhar, S., Patel, V.M., Nasrabadi, N.M. and Chellappa, R., 2014. Joint sparse representation for robust multimodal biometrics recognition. *IEEE Transactions on Pattern Analysis and Machine Intelligence*, 36(1), pp.113-126.
- [15] Mezai, L. and Hachouf, F., 2015. Score-level fusion of face and voice using particle swarm optimization and belief functions. *IEEE Transactions on Human-Machine Systems*, 45(6), pp.761-772.
- [16] Monwar, M.M. and Gavrilova, M., 2013. Markov chain method for multimodal biometric rank fusion. *Signal, Image and Video Processing*, 7(1), pp.137-149.
- [17] Liang, Y., Ding, X., Liu, C. and Xue, J.H., 2016. Combining multiple biometric traits with an order-preserving score fusion algorithm. *Neurocomputing*, 171, pp.252-261.
- [18] Poh, N. and Kittler, J., 2012. A unified framework for biometric expert fusion incorporating quality measures. *IEEE transactions on pattern analysis and machine intelligence*, 34(1), pp.3-18.
- [19] Nguyen, K., Denman, S., Sridharan, S. and Fookes, C., 2015. Score-level multibiometric fusion based on Dempster-Shafer theory incorporating uncertainty factors. *IEEE Transactions on Human-Machine Systems*, 45(1), pp.132-140.
- [20] Poh, N. and Kittler, J., 2012. A unified framework for biometric expert fusion incorporating quality measures. *IEEE transactions on pattern analysis and machine intelligence*, 34(1), pp.3-18.
- [21] Kumar, A. and Kumar, A., 2016. Adaptive management of multimodal biometrics fusion using ant colony optimization. *Information Fusion*, 32, pp.49-63.
- [22] Tao, Q., 2009. Face verification for mobile personal devices. University of Twente [Host].
- [23] Lee, H.C., Park, K.R., Kang, B.J. and Park, S.J., 2009, December. A new mobile multimodal biometric device integrating finger vein and fingerprint recognition. In *Ubiquitous Information Technologies & Applications, 2009. ICUT'09. Proceedings of the 4th International Conference on*(pp. 1-4). IEEE.
- [24] Yang, J. and Zhang, X., 2012. Feature-level fusion of fingerprint and finger-vein for personal identification. *Pattern Recognition Letters*, 33(5), pp.623-628.
- [25] Murphy, R.R., 1996. Biological and cognitive foundations of intelligent sensor fusion. *IEEE Transactions on Systems, Man, and Cybernetics, Part A: Systems and Humans*, 26(1), pp.42-51.
- [26] Smarandache, F., Dezert, J. (2006), "Proportional conflict redistribution rules for information fusion" in *Advances and Application on DSm T for Information Fusion (Collected Works)*, American Research Press, Rehoboth, 2, 3-68.
- [27] Daugman, J. G. (2004). How iris recognition works. *IEEE Trans. Circuits Sys. Video Tech.*, 14(1), 21–30.
- [28] Ravi, J., Raja, K. B., Venugopal, K. R. (2010). Fingerprint Recognition Using Minutia Score Matching. *CoRR* abs/1001.4186.
- [29] Surya, N., bhava Narayana, K., Sathish, K. (2013). Removal of False Minutiae Using Fuzzy Rules. *International Journal of Engineering And Science*, 3(6), 56-62.

- [30] Denoeux, T., Masson, M. (2010). Dempster-Shafer reasoning in large partially ordered sets: Applications in machine learning. *Integrated Uncertainty Management and Applications, Advances in Intelligent and Soft Computing*, New York, NY, USA: Springer-Verlag, 68, 39–54.
- [31] Civicioglu, P. (2013). Backtracking Search Optimization Algorithm for numerical optimization problems. *Applied Mathematics and Computation*, 219(15), 8121-8144.
- [32] Kumar, A., Passi, A. (2010). Comparison and combination of iris matchers for reliable personal authentication. *Pattern Recognition* 43(3), 1016-1026.
- [33] Tome, P. et al. (2015). The 1st Competition on Counter Measures to Finger Vein Spoofing Attacks, In: *International Conference on Biometrics (ICB)*, Phuket, pp513-518.
- [34] Cappelli, R., Ferrara, M., Franco, A., Maltoni, D. (2007). Fingerprint verification competition 2006. *Biometric Technology Today*, 15(7-8), 7-9.
- [35] Srinivas, N., Veeramachaneni, K., Osadciw, L. A. (2009). Fusing correlated data from multiple classifiers for improved biometric verification. *Information Fusion. FUSION'09. 12th International Conference on*, Seattle, WA, 1504-1511.
- [36] Zhang, L., Zhang, D., Guo, Z. (2012). Phase congruency induced local features for fingerknuckle-print recognition. *Pattern Recognition*, 45(7), 2522-2531.
- [37] Kittler, J., Hatef, M., Duin, R. P., & Matas, J. (1998). On combining classifiers. *IEEE transactions on pattern analysis and machine intelligence*, 20(3), 226-239.
- [38] Mohi-ud-Din, S. G., Bin Mansoor, A., Masood, H., Mumtaz, M. (2011). Personal identification using feature and score level fusion of palm and finger-prints. *Signal Image Video Process*, 5, 477–483.
- [39] Oussalah, M., Schutter, J. D. (2003). On the use of Hamacher's t-norms family for information aggregation. *Inf. Sci.*, 153(1), 107–154.